

Proper Generalized Decomposition of LCM models

F. Chinesta¹, A. Leygue¹, A. Poitou¹, S. Chatel², S. Garcia³ and LL. Gascon³

¹*EADS Foundation International Chair, GEM, Ecole Centrale Nantes, BP 92101, F-44321 Nantes cedex 3, France, francisco.chinesta@ec-nantes.fr*

²*EADS France Innovation Works, Allée du Chaffault, 44340 Bouguenais, France, sylvain.chatel@eads.net*

³*Universidad Politécnica de Valencia, Camino de Vera s/n, E-46071 Valencia, Spain, jugarcia@mcm.upv.es*

ABSTRACT: Simulation of RTM processes is usually performed in 2D. Thus, only a mesh of the middle plane is needed with the associated degrees of freedom leading to important savings with respect to fully 3D modeling. However such modeling needs the definition of an equivalent in-plane permeability representing the ignored dimension (the thickness). The definition of such permeability is not a trivial task because each ply in the thickness direction can be anisotropic, the principal anisotropy directions being different from one ply to the neighbor plies. In this work we propose a novel fully 3D modeling whose computational cost is equivalent to a 2D solution. It allows addressing properly the equivalent in-plane permeability issue.

KEYWORDS: RTM, Permeability, Separated representations, Model reduction

INTRODUCTION

In general the simulation of RTM processes assumes a 2D flow model. The most usual model results of combining the Darcy's law and the flow incompressibility:

$$\begin{cases} \mathbf{v} = -\mathbf{K} \cdot \nabla p \\ \nabla \cdot \mathbf{v} = 0 \end{cases}$$

that results in the second order BVP:

$$\nabla \cdot (\mathbf{K} \cdot \nabla p) = 0$$

The main issue in defining this model concerns the definition of the permeability tensor \mathbf{K} . Different techniques exist, but in what follows we are assuming that an averaged permeability has been determined for each type of reinforcement architecture.

PGD IN PLATE DOMAINS

In what follows we are illustrating the construction of the Proper Generalized Decomposition of a model defined in a plate domain $\Xi = \Omega \times I$ with $\Omega \subset \mathbb{R}^2$ and $I = [0, H]$:

$$\nabla \cdot (\mathbf{K} \cdot \nabla p) = 0 \tag{1}$$

We consider that the laminate is composed of P different anisotropic plies each one characterized by a well defined permeability tensor $\mathbf{K}_i(x, y)$ -it is assumed constant in

the ply thickness-. Moreover, without a loss of generality, we assume the same thickness for the different layers of the laminate that we denote by h . Thus, we can define a characteristic function representing the position of each layer:

$$\chi_i(z) = \begin{cases} 1 & z_i \leq z \leq z_{i+1}, \quad i = 1, \dots, P \\ 0 & \text{otherwise} \end{cases} \quad (2)$$

where $z_i = (i-1) \times h$. Now, the laminated permeability can be given in the following separated form:

$$\mathbf{K}(x, y, z) = \sum_{i=1}^{i=P} \mathbf{K}_i(\mathbf{x}) \cdot \chi_i(z) \quad (3)$$

where $\mathbf{x} = (x, y) \in \Omega$. The weak form of Eq. (1) writes:

$$\int_{\Xi} \nabla p^* \cdot (\mathbf{K} \cdot \nabla p) d\Xi = 0 \quad (4)$$

with the test function p^* in an appropriate functional space. The solution $p(x, y, z)$ is searched under the separated form:

$$p(\mathbf{x}, z) \approx \sum_{i=1}^{i=N} X_i(\mathbf{x}) \cdot Z_i(z) \quad (5)$$

In what follows we are illustrating the construction of one such decomposition. For this purpose we assume that at iteration $n < N$ the solution is already known:

$$p^n(\mathbf{x}, z) = \sum_{i=1}^{i=n} X_i(\mathbf{x}) \cdot Z_i(z) \quad (6)$$

and that at the present iteration we look for the solution enrichment:

$$p^{n+1}(\mathbf{x}, z) = p^n(\mathbf{x}, z) + R(\mathbf{x}) \cdot S(z) \quad (7)$$

The test function involved in the weak form is searched under the form:

$$p^*(\mathbf{x}, z) = R^*(\mathbf{x}) \cdot S(z) + R(\mathbf{x}) \cdot S^*(z) \quad (8)$$

By introducing Eqs. (7) and (8) into (4) it results:

$$\int_{\Xi} \left(\left(\begin{array}{c} \tilde{\nabla} R^* \cdot S \\ R^* \cdot \frac{dS}{dz} \end{array} \right) + \left(\begin{array}{c} \tilde{\nabla} R \cdot S^* \\ R \cdot \frac{dS^*}{dz} \end{array} \right) \right) \cdot \left(\mathbf{K} \cdot \left(\begin{array}{c} \tilde{\nabla} R \cdot S \\ R \cdot \frac{dS}{dz} \end{array} \right) \right) d\Xi = - \int_{\Xi} \left(\left(\begin{array}{c} \tilde{\nabla} R^* \cdot S \\ R^* \cdot \frac{dS}{dz} \end{array} \right) + \left(\begin{array}{c} \tilde{\nabla} R \cdot S^* \\ R \cdot \frac{dS^*}{dz} \end{array} \right) \right) \cdot \mathbf{Q}^n d\Xi \quad (9)$$

where $\tilde{\nabla}$ denotes the plane component of the gradient operator $\tilde{\nabla}^T \equiv (\partial/\partial x, \partial/\partial y)$ and \mathbf{Q}^n denotes the flux at iteration n :

$$\mathbf{Q}^n = \mathbf{K} \cdot \sum_{i=1}^{i=n} \left(\begin{array}{c} \tilde{\nabla} X_i(\mathbf{x}) \cdot Z_i(z) \\ X_i(\mathbf{x}) \cdot \frac{dZ_i(z)}{dz} \end{array} \right) \quad (10)$$

Now, as the enrichment process is non-linear we propose to search the couple of functions $R(\mathbf{x})$ and $S(z)$ by applying an alternating direction fixed point algorithm. Thus, assuming $R(\mathbf{x})$ known, we compute $S(z)$, and then we update $R(\mathbf{x})$. The process continues until reaching convergence. The converged solutions allow defining the next term in the finite sums decomposition: $R(\mathbf{x}) \rightarrow X_{n+1}(\mathbf{x})$ and $S(z) \rightarrow Z_{n+1}(z)$.

We are illustrating each one of the just referred steps:

1. Computing $R(\mathbf{x})$ from $S(z)$:

When $S(z)$ is known the test function reduces to:

$$p^*(\mathbf{x}, z) = R^*(\mathbf{x}) \cdot S(z) \quad (11)$$

and the weak form (9) reduces to:

$$\int_{\Xi} \begin{pmatrix} \tilde{\nabla} R^* \cdot S \\ R^* \cdot \frac{dS}{dz} \end{pmatrix} \cdot \mathbf{K} \cdot \begin{pmatrix} \tilde{\nabla} R \cdot S \\ R \cdot \frac{dS}{dz} \end{pmatrix} d\Xi = - \int_{\Xi} \begin{pmatrix} \tilde{\nabla} R^* \cdot S \\ R^* \cdot \frac{dS}{dz} \end{pmatrix} \cdot \mathbf{Q}^n d\Xi \quad (12)$$

Now, as all the functions involving the coordinate z are known, they could be integrated in $I = [0, H]$. Thus, if we consider:

$$\mathbf{K} = \begin{pmatrix} \mathbb{k} & \mathbf{k} \\ \mathbf{k}^T & \kappa \end{pmatrix} \quad (13)$$

with $\mathbb{k} = \begin{pmatrix} k_{xx} & k_{xy} \\ k_{yx} & k_{yy} \end{pmatrix}$, $\mathbf{k} = \begin{pmatrix} k_{xz} \\ k_{yz} \end{pmatrix}$ and $\kappa = k_{zz}$, then we can define:

$${}^x \mathbf{K} = \begin{pmatrix} \int_{z=0}^{z=H} \mathbb{k} S^2 dz & \int_{z=0}^{z=H} \mathbf{k} \frac{dS}{dz} S dz \\ \int_{z=0}^{z=H} \mathbf{k}^T \frac{dS}{dz} S dz & \int_{z=0}^{z=H} \kappa \left(\frac{dS}{dz} \right)^2 dz \end{pmatrix} \quad (14)$$

and

$${}^x \mathbf{Q}^n = \sum_{i=1}^{i=N} \begin{pmatrix} \int_{z=0}^{z=H} \mathbb{k} S Z_i dz & \int_{z=0}^{z=H} \mathbf{k} S \frac{dZ_i}{dz} dz \\ \int_{z=0}^{z=H} \mathbf{k}^T \frac{dS}{dz} Z_i dz & \int_{z=0}^{z=H} \kappa \frac{dS}{dz} \frac{dZ_i}{dz} dz \end{pmatrix} \begin{pmatrix} \tilde{\nabla} X_i(\mathbf{x}) \\ X_i(\mathbf{x}) \end{pmatrix} \quad (15)$$

that allows writing equation (12) into the form

$$\int_{\Omega} \begin{pmatrix} \tilde{\nabla} R^* \\ R^* \end{pmatrix} \cdot \begin{pmatrix} {}^x \mathbf{K} \cdot \begin{pmatrix} \tilde{\nabla} R \\ R \end{pmatrix} \end{pmatrix} d\Omega = - \int_{\Omega} \begin{pmatrix} \tilde{\nabla} R^* \\ R^* \end{pmatrix} \cdot {}^x \mathbf{Q}^n d\Omega \quad (16)$$

that defines an elliptic 2D problem defined in the middle plane of the plate.

2. Computing $S(z)$ from $R(\mathbf{x})$:

When $R(\mathbf{x})$ is known the test function writes:

$$p^*(\mathbf{x}, z) = R(\mathbf{x}) \cdot S^*(z) \quad (17)$$

and the weak form (9) reduces to:

$$\int_{\Xi} \begin{pmatrix} \tilde{\nabla} R \cdot S^* \\ R \cdot \frac{dS^*}{dz} \end{pmatrix} \cdot \mathbf{K} \cdot \begin{pmatrix} \tilde{\nabla} R \cdot S \\ R \cdot \frac{dS}{dz} \end{pmatrix} d\Xi = - \int_{\Xi} \begin{pmatrix} \tilde{\nabla} R \cdot S^* \\ R \cdot \frac{dS^*}{dz} \end{pmatrix} \cdot \mathbf{Q}^n d\Xi \quad (18)$$

Now, as all the functions involving the in-plane coordinates $\mathbf{x} = (x, y)$ are known, they could be integrated in Ω . Thus, using the previous notation, we can define:

$${}^z\mathbf{K} = \begin{pmatrix} \int_{\Omega} (\tilde{\nabla}R) \cdot (\mathbb{k} \cdot (\tilde{\nabla}R)) d\Omega & \int_{\Omega} (\tilde{\nabla}R) \cdot \mathbf{k} R d\Omega \\ \int_{\Omega} \mathbf{k} \cdot (\tilde{\nabla}R) R d\Omega & \int_{\Omega} \kappa(R)^2 d\Omega \end{pmatrix} \quad (19)$$

and

$${}^z\mathbf{Q}^n = \sum_{i=1}^{i=N} \begin{pmatrix} \int_{\Omega} \tilde{\nabla}R \cdot (\mathbb{k} \cdot \tilde{\nabla}X_i) d\Omega & \int_{\Omega} \tilde{\nabla}R \cdot \mathbf{k} X_i d\Omega \\ \int_{\Omega} R \mathbf{k} \cdot \tilde{\nabla}X_i d\Omega & \int_{\Omega} \kappa R X_i d\Omega \end{pmatrix} \begin{pmatrix} Z_i \\ \frac{dZ_i}{dz} \end{pmatrix} \quad (20)$$

that allows writing equation (18) into the form

$$\int_I \begin{pmatrix} S^* \\ \frac{dS^*}{dz} \end{pmatrix} \cdot \left({}^z\mathbf{K} \cdot \begin{pmatrix} S \\ \frac{dS}{dz} \end{pmatrix} \right) dz = - \int_I \begin{pmatrix} S^* \\ \frac{dS^*}{dz} \end{pmatrix} \cdot {}^z\mathbf{Q}^n dz \quad (21)$$

that defines a one-dimensional BVP.

FLOW IN A 2-LAYERS DOMAIN

In order to illustrate the method presented above, we compute the Darcy flow in a thin plate composed of two superposed transversely isotropic layers with different orientation. As shown in Fig. 1, we consider a plate of dimensions $L > l \gg h > 0$ along the x, y and z axis respectively where we impose a pressure gradient along the x axis through the imposed inlet and outlet pressures: P_{in} and P_{out} . Zero fluxes boundary conditions are imposed along the upper, lower and lateral boundaries.

In each layer the permeability tensor \mathbf{K} is defined as:

$$\mathbf{K} = K_{\parallel} \mathbf{1} \times \mathbf{1} + K_{\perp} (\boldsymbol{\delta} - \mathbf{1} \times \mathbf{1}) \quad (22)$$

Where $\mathbf{1}$ is the medium principal direction and K_{\parallel} and K_{\perp} respectively are the scalar permeabilities along $\mathbf{1}$ and perpendicular to $\mathbf{1}$. We set the principal directions respectively to $+45^\circ$ and -45° with respect to the x axis the in the upper and lower layer, i.e. :

$$\begin{aligned} \mathbf{1}^{\text{upper}} &= \left(\frac{\sqrt{2}}{2}, \frac{\sqrt{2}}{2}, 0 \right)^T \\ \mathbf{1}^{\text{lower}} &= \left(\frac{\sqrt{2}}{2}, -\frac{\sqrt{2}}{2}, 0 \right)^T. \end{aligned} \quad (23)$$

For the scalar permeabilities, we take $\frac{K_{\parallel}}{K_{\perp}} = 10$.

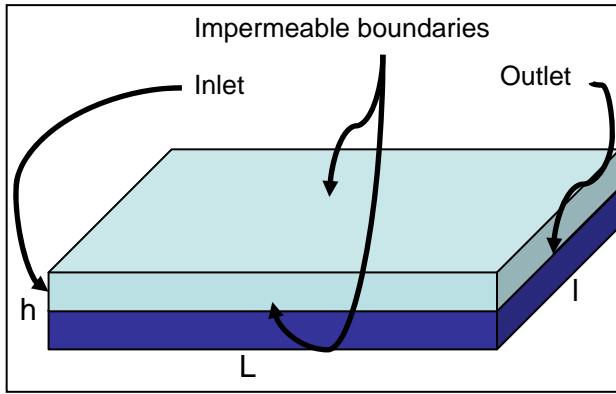


Figure 1 : Thin plate Geometry

The solution of this problem using a fully three dimensional finite element description can be found in the PhD dissertation of F. Loix [3].

In the (x, y) plane, we solve the elliptic 2D problem defined by Eq. (16) using a Galerkin Finite Elements method with P1 triangular elements. The two-dimensional mesh used in-plane has a constant spacing in the x direction but is refined in the y direction, close to the lateral boundaries of the domain. In the z direction we solve the BVP defined by Eq. (21) using a 1D Finite Element description with linear interpolation on a uniform 1D mesh. Table 1 summarizes the precise numerical values used in this example as well as the finite elements mesh parameters.

To initialize the PGD iterations, we pick the first mode of the solution $(X_1(\mathbf{x}), Z_1(z))$ as:

$$\begin{aligned} X_1(\mathbf{x}) &= P_{\text{out}} + (P_{\text{out}} - P_{\text{in}}) \left(\frac{x}{L} - 1 \right) \\ Z_1(z) &= 1 \end{aligned} \quad (24)$$

which is the solution of the z -averaged problem. Additional modes have been computed as described in section 2 until the norm of the final residual was less than 1% of the norm of the residual when only the first mode is considered.

Table 1: Numerical parameters

Physical dimensions	Value	Units
L	1	m
l	0.2	m
h	0.01	m
K_{\parallel}	10^{-7}	m^2
K_{\perp}	10^{-8}	m^2
P_{in}	1.05	bar
P_{out}	1.00	bar
Mesh Parameters	# dof	# elements
(x, y) -plane	1500	2842
z -axis	21	20

The first mode actually describes very well the final pressure solution, excepted close to the boundaries. Therefore, only 21 additional modes are computed by the PGD method, mostly to satisfy the imposed boundary conditions. Nevertheless, these additional modes have a dramatic influence on the flow patterns, as illustrated below. Finally, although the equivalent three-dimensional problem would involve more than 30000 unknowns, the additional modes are computed in a few seconds as the computational cost of the method scales like the cost of a two dimensional modeling (16).

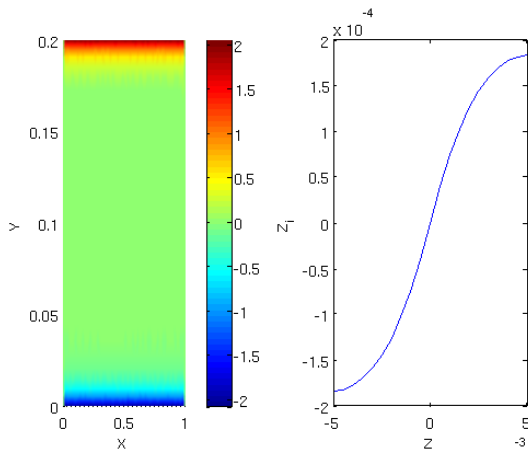


Figure 2: Second mode of the PGD solution $X_2(x, y)$ and $Z_2(z)$.

In Fig. 2, we show the second mode: $(X_2(\mathbf{x}), Z_2(z))$. As the first mode does not satisfy the zero flux boundary conditions, the second mode provides a local correction. A careful analysis of the modes would also show that a later mode provides another correction to the pressure field close to the inlet and outlet of the plate, to accommodate the Dirichlet boundary conditions.

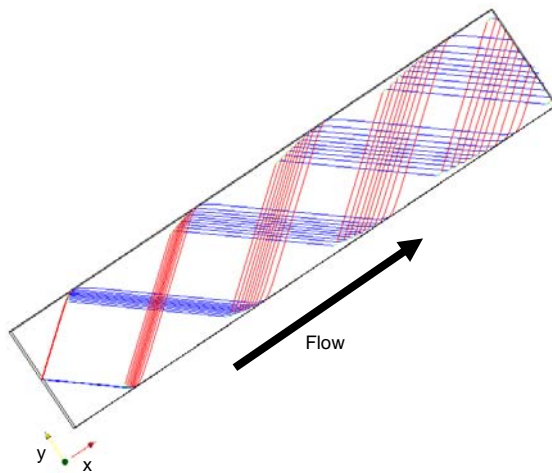


Figure 3: Streamlines of points initially located on a vertical line in the middle of the inlet face

In Fig. 3, we illustrate the complex mass transfer taking place between the two layers by showing the path-lines of material points initially located on a vertical line in the centre of the inlet. Due to the anisotropy, these points travel towards the lateral boundaries in orthogonal directions, depending on the layer to which they belong. At the lateral

boundaries, these points are forced to switch layer as a result from the zero flux condition. The path-lines therefore organize into a set of flattened spirals. Such 3D effects are of course impossible to predict using purely two-dimensional models but are well captured in the separated representation that we use.

CONCLUSIONS

This paper revisits a recurrent issue in the numerical modeling of RTM flows, the one related to the pertinence of using 2D flow models making use of an averaged permeability of the different layers involved in the laminate. In complex situations significant deviations could be found, these deviations are being studied at present, and could justify the use of a fully 3D modeling. However, 3D simulations are reputed expensive from the point of view of the computational resources required for addressing complex scenarios, in which many plies are involved in the composite laminated. The use of separated representations as the ones involved in the proper generalized decompositions –PGD– could be an appealing alternative for addressing 3D models with a cost characteristic of 2D simulations. The application of the PGD on the fully 3D simulations of flows encountered in RTM processes, involving a moving front, constitutes a work in progress.

REFERENCES

- [1] A. Ammar, B. Mokdad, F. Chinesta, R. Keunings, A new family of solvers for some classes of multidimensional partial differential equations encountered in kinetic theory modeling of complex fluids, *J. Non-Newtonian Fluid Mech.*, 139: 153-176, 2006.
- [2] A. Ammar, B. Mokdad, F. Chinesta, R. Keunings, A new family of solvers for some classes of multidimensional partial differential equations encountered in kinetic theory modeling of complex fluids. Part II: transient simulation using space-time separated representations, *J. Non-Newtonian Fluid Mech.*, 144: 98-121, 2007.
- [3] F. Loix, Modelling of transport phenomena in porous media. *PhD dissertation*, Université catholique de Louvain, 2005.